

SMA observations of massive star forming regions

Sheng-Yuan Liu¹ and the SMA Team^{1,2}

¹Academia Sinica Institute of Astronomy and Astrophysics,
P.O. Box 23-141, Taipei 106, Taiwan, R.O.C.
email: sylu@asiaa.sinica.edu.tw

²Harvard-Smithsonian Center for Astrophysics,
60 Garden Street, Cambridge, MA 02138, U.S.A.

Abstract. The Submillimeter Array located atop of Mauna Kea in Hawaii is a collaborative project of the Smithsonian Astrophysical Observatory and the Academia Sinica Institute of Astronomy and Astrophysics. The high angular resolution provided by the SMA is particularly suitable for studying massive star-forming cores which often exhibit strong (sub)millimeter continuum and spectral features but mostly locate within crowded regions at large distances. We report the latest SMA status and recent results in the area of massive star formation obtained with the array.

Keywords. interferometers; high angular resolution; HII regions; jets and outflows; molecules

1. Introduction

The Submillimeter Array (SMA) is a collaborative project of the Smithsonian Astrophysical Observatory (SAO) and the Academia Sinica Institute of Astronomy and Astrophysics (ASIAA). With its initial concept conceived at the SAO in 1983, the project identified Mauna Kea as the observatory site and the construction started in the early 1990s. In 1996, ASIAA joined the project by expending the original six-element array into an eight-element array, nearly doubling the imaging speed. By the end of 2003, all eight elements of the SMA were deployed on top of Mauna Kea. The SMA was formally dedicated on 2003 November 22, by which time regular operation phase started. Table 1 gives a list of basic characteristics of the array.

In studying massive star formation, many key questions remain to be answered. For example, what are the initial conditions/environments within which massive stars form?

Table 1. The Basic Characteristics of the SMA

Antennas	Eight reflectors, 6 meters in diameter Carbon Fiber backup structure, Machined cast aluminum panels Primary reflector $f/0.4$, surface $12\mu\text{m}$ rms, Chopping secondary reflector
Configurations	4 rings, 24 pads, up to 8 antennas per ring
Baselines	8 to 508 meters (15-250 meters with current pads)
Frequencies	180 to 900 GHz (current bands: 175-255, 250-350, 600-720 GHz)
Receivers	up to 8 per cryostat (simultaneous dual bands/polarizations)
Correlator	Flexible Hybrid analog-digital design up to 2 GHz bandwidths, 2 receivers, 8 stations
Filed of View	70 to 14 arcsec
Resolution	0.5 to 0.1 arcsec
Sensitivity	for 1mm H ₂ O, 8hr, 2GHz bandwidth: $\Delta S \sim 0.4, 1, 10$ mJy at 230, 345, and 690 GHz

How general are the outflow and disk phenomena associated with young stellar objects toward the massive end of their mass spectrum? Where and how these outflows get launched and regulated? How these disks might evolve? Given their rapid evolution, young massive stars are likely to be deeply emdeded in the natal clouds. Dust surrounding these objects thus absorbs almost all stellar radiation and reradiates in the far-infrared and submillimeter wavelengths, while the surrounding dense and warm molecular gas also exhibits intense submillimeter line emission. The SMA therefore provides the crucial resolving power in particular for studying massive star-forming cores which mostly locate within crowded regions at large distances. We report results from observations obtained with the SMA in the field of massive star formation during its early commissioning phase as well as the recent regular operation seasons.

2. Recent Results

2.1. G5.89-0.39

G5.89-0.39 is a shell-like ultracompact (UC) HII region (Wood & Churchwell 1989) at a distance of ~ 2 kpc associated with a molecular outflow (e.g. Acord *et al.* 1997). Sollins *et al.* (2004) mapped G5.89-0.39 and its surroundings with the SMA at $2.8'' \times 1.8''$ angular resolution in 1.3 mm continuum, SiO 5–4 and eight other molecular lines. The molecular outflow is resolved for the first time and is definitely bipolar. The SiO 5–4 position-velocity structure with emission exceeding 30 km s^{-1} suggests the outflow is mainly in the plane of the sky and highly energetic. The 1.3 mm continuum is likely the outflow driving source as its peak lies on the projected outflow axis, halfway between the peaks of the two outflow lobes. In addition, the slightly extended continuum emission seems to show a physical connection to both outflow lobes in the form of extensions along the outflow axis.

2.2. IRAS 18089-1732

IRAS 18089-1732, at a distance of ~ 3.6 kpc with $10^{4.5} L_{\odot}$ in luminosity, is one of the young high-mass protostellar object (HMPO) among the sample of 69 HMPOs selected and surveyed by Sridharan *et al.* (2002). Past observations revealed a massive core greater than $2000 M_{\odot}$ in millimeter continuum associated with maser emission and weak 3.6 cm radio continuum (Beuther *et al.* 2002b, 2002d). Observations with the SMA at 217 and 344 GHz by Beuther *et al.* 2004a, 2004b detected a total of 34 molecular lines from 16 molecules/isotopomers, supporting the hot-core nature of this object. The large number of observed HCOOCH₃ lines allowed an estimate of the temperature for the central region to be 350 ± 100 K (Beuther *et al.* 2004a). The SiO 5–4 data show a collimated outflow in the northern direction. In contrast, the HCOOCH₃ 20–19 line, which traces high-density gas, is confined to the very center of the region and shows a velocity gradient across the core, most likely originating from a rotating disk that is influenced by outflows and infall (beuther04b). The combined evidence supports the scenario in which high-mass stars form via disk accretion accompanies by collimated jets/outflows, just in a similar fashion as their low-mass counterparts.

2.3. IRAS 20126+4104

IRAS 20126+4104 is the first high-mass protostellar object identified with a jet and a disk. The SiO and HCO⁺ emission has been observed tracing a well collimated bipolar jet/outflow located symmetrically around the central YSO (Cesaroni *et al.* 1997, 1999). Images in the highly excited CO 7–6 line also exhibit two hot spots near the tip of the SiO jet (Kawamura *et al.* 1999). The hot spots, separated by about $20''$, coincide with the H2

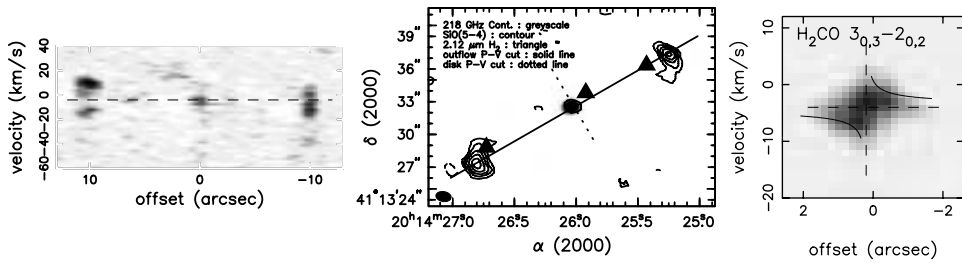


Figure 1. Left panel: position-velocity diagram of SiO 5-4 emission along the jet/outflow. Middle panel: 1.3 mm continuum and integrated SiO 5-4 emission of IRAS 20126+4104. Right panel: position-velocity diagram of H₂CO 3_{0,3} – 2_{0,2} emission along the disk.

knots (Shepherd *et al.* 2000). Perpendicular to the jet/outflow, both the CH₃CN as well as the NH₃ (1,1) and (2,2) lines show an elongated disk-like structure with its velocity field consistent with Keplerian rotation (Cesaroni *et al.* 1997, 1999; Zhang, Hunter, & Sridharan 1998). Imaged with the SMA by Liu *et al.* the integrated SiO 5-4 emission at 217 GHz depicts a clear bow-shock morphology coinciding with the H₂ emission. The emission location suggests SiO is mostly concentrated/excited immediately behind the bow shock apex. The “tail” morphology appears extending in the direction of the jet precession. Along the disk direction, the position-velocity diagrams of the K=0 and K=2 H₂CO lines at 218 GHz suggest spin-up motions, most likely associated with Keplerian rotation. Moreover, a rich chemistry exists in both the core/disk and the outflow — in addition to H₂CO, CH₃OH, DCN, and HC₃N were all detected toward the central YSO. In the outflow, while SiO emission appears to be stronger toward the SE knot, little H₂CO or CH₃OH emission was detected. In contrast, SiO, H₂CO, and CH₃OH were detected toward the NW knot with their peaks progressively located away from the bow shock tip.

2.4. Cepheus A-East

Within a molecular complex associated with Cepheus OB3 some 725 pc away, the Cepheus A region displays various star formation signatures (Torrelles *et al.* 1993). For example, multiple outflows on different scales have been found (Rodríguez *et al.* 1980; Ho, Moran, & Rodríguez 1982; Hayashi, Hasegawa, & Kaifu 1988). In Cepheus A East, no less than sixteen radio-continuum sources were detected (Hughes & Wouterloot 1984; Garay *et al.* 1996). Among these, HW2 is suggested to be the driving source for the molecular outflows. Using the SMA at 343 GHz with an angular resolution of $\sim 1.5''$, Brogan *et al.* (private communication) detected submillimeter counterparts of the radio sources HW2, HW3b, and HW3c. Numerous lines from hot core tracing species, such as CH₃OH, CH₂CO, HCOOCH₃, CH₃OCH₃, and C₂H₅CN are all detected toward the HW2 core.

2.5. IRAS 05358+3543

IRAS 05358+3543, at a distance of 1.8 kpc, is another massive star forming object among the 69 HMPO sample studied by Sridharan *et al.* (2002). Both H₂O and CH₃OH masers have been detected in this region (Tofani *et al.* 1995; Minier *et al.* 2000). Similar to Cepheus A East, multiple outflows have also been imaged in CO (Beuther *et al.* 2002a). The SMA observations carried out by Beuther *et al.* (private communication) successfully imaged dust condensations in this region at 338 GHz as well as line emission from various complex molecules. The large number of detected CH₃OH lines at 348 GHz are used for temperature and density analysis (see Leurini *et al.* 2005 in this volume).

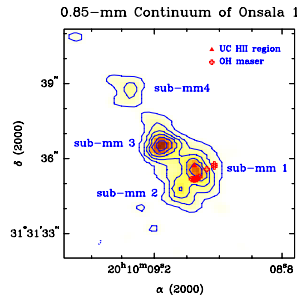


Figure 2. 850 μm continuum of Onsala 1 shown in both contours and grayscale.

2.6. *Onsala 1*

Given its compactness, Onsala 1 is one of the smallest, hence possibly the youngest UCHII regions in the Galaxy. Located at a distance of 1.8 kpc, its physical size would be around 0.01 pc, implying a very young age of 1000 years. H_2O and OH maser emission, has also been found in this region (Downes *et al.* 1979; Ho *et al.* 1983). At an angular resolution of $0.6''$, recent 345 GHz SMA observations by Su *et al.* (private communication) revealed at least four components (denoted as sub-mm 1-4) within a $5''$ field (i.e., 0.05 pc). Sub-mm 1 appears associated with the UC HII region and OH masers and is dominated by free-free emission from ionized gas as recent VLA continuum observations at 3.6 and 1.3 cm suggested. In contrast, the newly identified sub-mm 2, 3, and 4 appear to be dominated by dust emission with no radio counterpart. Furthermore, sub-mm 2 & 3 are spatially coincident with H_2O maser spots (Zheng *et al.* 1985), indicating both are likely hot core candidates, which represent the sites of high-mass star formation prior to the UC HII region phase. The results strongly suggest that Onsala 1 harbors massive stars at different but extremely young evolutionary stages in their formation.

2.7. *Orion KL*

At a distance of 450 pc, Orion KL is the nearest and most studied region of massive star formation. The region exhibits a complex cluster of near- to mid-infrared sources (e.g. Dougados *et al.* 1993; Greenhill *et al.* 2004). At least two outflows at different scales are observed originating from this region: one large scale high-velocity outflow in the southeast-northwest direction (e.g., Allen & Burton 1993; Wright *et al.* 1995; Schultz *et al.* 1999) and at a smaller scale one lower velocity outflow in the northeast-southwest direction (e.g., Genzel & Stutzki 1989; Blake *et al.* 1996; Chrysostomou *et al.* 1997; Stolovy *et al.* 1998). The driving source(s) of the outflows are, however, uncertain. Possible candidates are the radio sources I and/or the infrared source n, also known as radio source L (Menten & Reid 1995).

SMA observations by Beuther *et al.* (2004c, 2005) at 338 and 348 GHz detected about 145 spectral lines from 25 species/isotopologues at different vibrationally excited states. Chemical differentiation within the region is evident as reported by past studies: most nitrogen bearing molecules are strong toward the hot core, whereas oxygen-bearing molecules peak toward the south-west in the so-called compact ridge. The SiO lines, in particular, are found to trace the collimated low-velocity molecular jet emanating from source I as well as larger-scale emission likely associated with a different outflow.

The 850 μm continuum image resolved source I from the hot core and detected, for the first time, source n at a wavelength shorter than 7 mm. Furthermore, a new continuum peak between the sources I and n, SMA1, is also found. The radio source I lies close to the center of a biconical outflow traced by SiO and H_2O maser emission (Gezari 1992;

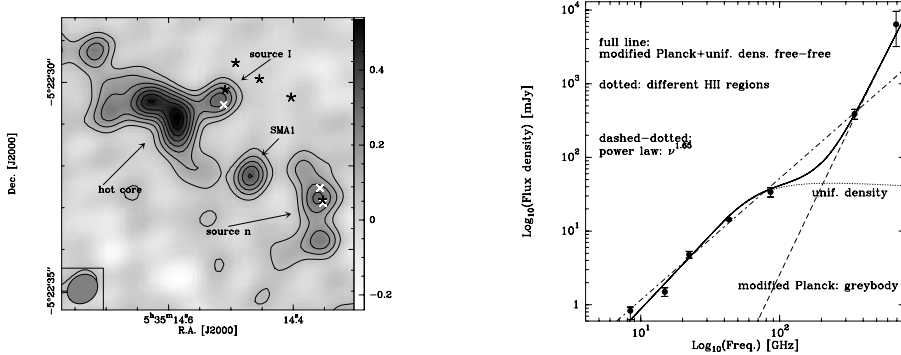


Figure 3. Left Panels: submillimeter continuum of Orion KL at 850 μm shown in both contours and grayscale. Right panel: The SED from 8 to 690 GHz for source I in Orion KL (From H. Beuther, private communication)

Menten & Reid 1995; Greenhill *et al.* 2004). Its spectral energy distribution (SED) from 8 to 86 GHz can be explained by optically thick free-free emission. With the new measurement, the SED for source I from 8 to 348 GHz allows two equally possible interpretations. One possibility is to fit the lower frequency part of the spectrum with proton-electron free-free emission, but to allow dust emission to dominate the submillimeter continuum. Alternatively, one can also fit a power law $S \propto \nu^\alpha$ to the SED with $\alpha \sim 1.65 \pm 0.2$. This is similar to the spectral index observed toward Mira variable stars (Reid & Menten 1997). Supporting evidence that the radio continuum forms under Mira-like conditions in a region with a temperature ~ 1600 K and a density of $10^{11} - 10^{12} \text{ cm}^{-3}$ comes from the detection of SiO masers from source I.

The highlight comes from observations toward Orion KL at 680 and 690 GHz during a recent high frequency band campaign. Through visibility fitting, a constraint on the source I flux density at 440 μm of 6.4 ± 3.2 Jy is derived. The combined SED from 8 to 690 GHz clearly discriminates between the two models mentioned above and identifies source I as a deeply embedded protostellar object with optical thick free-free emission up to 100 GHz plus dust emission accounting for most of its submm flux. The 650 GHz observations also confirmed SMA1 to be an independent protostellar source rather than an extension of the hot core. Finally, 24 spectral line features are observed in the bandpass, with a large fraction of lines undetected in previous single-element line survey (Schilke *et al.* 2001). Molecular emission from highly excited lines such as CH_3CN 37₂ – 36₂, CH_3OH 22₁ – 21₂, and SO_2 35_{3,33} – 34_{2,32} all shows peaks toward source I, SMA1, and the hot core location, indicating dense and warm gas surrounding these objects.

3. Future Prospects

As regular science programs carry on, instrumental upgrades will continue to realize SMA's full capability. Among many items, efforts in the near future include the installation of receivers for simultaneous dual polarization capability, the link-up with the James Clerk Maxwell Telescope and the Caltech Submillimeter Observatory for sensitivity improvement, as well as the development of the remaining receiver bands for a complete frequency coverage.

Acknowledgements

The authors thank H. Beuther, Y.-N. Su, C. L. Brogan, and P. K. Sollins for discussing their results and providing the images in this paper. We also thank the whole SMA

team from both SAO and IAA for their dedicated and continuous work in making this instrument possible.

References

- Acord, J.M., Walmsley, C.M., & Churchwell, E., 1997 *ApJ*, 475, 693
- Allen, D.A., & Burton, M.G., 1993 *Nature*, 363, 54
- Beuther, H., Schilke, P., Gueth, F., McCaughrean, M., Andersen, M., Sridharan, T.K., & Menten, K.M., 2002a *A&A*, 387, 931
- Beuther, H., Schilke, P., Menten, K.M., Motte, F., Sridharan, T.K., & Wyrowski, F., 2002b *ApJ*, 566, 945
- Beuther, H., Schilke, P., Sridharan, T.K., Menten, K.M., Walmsley, C.M., & Wyrowski, F., 2002c *A&A*, 383, 892
- Beuther, H., Walsh, A., Schilke, P., Sridharan, T.K., Menten, K.M., & Wyrowski, F., 2002d *A&A*, 390, 289
- Beuther, H., Zhang, Q., Hunter, T.R. *et al.*, 2004a *ApJL*, 616, 19
- Beuther, H., Hunter, T.R., Zhang, Q. *et al.*, 2004b *ApJL*, 616, 23
- Beuther, H. Zhang, Q., Greenhill, L.J. *et al.*, 2004c *ApJL*, 616, 31
- Beuther, H. Zhang, Q., Greenhill, L.J. *et al.*, 2005 *ApJL*, accepted
- Blake, G.A., Mundy, L.G., Carlstrom, J. E., *et al.*, 1996 *ApJL*, 472, 49
- Cesaroni, R., Felli, M., Testi, L., Walmsley, C.M. & Olmi, L., 1997 *A&A*, 325, 725
- Cesaroni, R., Felli, M., Jenness, T., Neri, R., Robberto, M., Testi, L., & Walmsley, C.M., 1999 *A&A*, 345, 949
- Chrysostomou, A., Burton, M.G., Axon, D.J., *et al.*, 1997 *MNRAS*, 289, 605
- Dougados, C., Lena, P., Ridgway, S.T., Christou, J.C., & Probst, R. G., 1993 *ApJ*, 406, 112
- Downes, D., Genzel, R., Moran, J.M., Johnston, K.J., Matveenko, L.I., Kogan, L.R., Kostenko, V.I., & Ronnang, B., 1979 *A&A*, 79, 233
- Garay, G., Ramírez, S., Rodríguez, L.F., Curiel, S., & Torrelles, J.M., 1996 *ApJ*, 459, 193
- Genzel, R., & Stutzki, J., 1989 *ARA&A*, 27, 41
- Gezari, D.Y., 1992 *ApJL*, 396, 43
- Greenhill, L. J., *et al.* 2004 *ApJL*, 605, 57
- Hayashi, S.S., Hasegawa, T., & Kaifu, N., 1988 *ApJ*, 332, 354
- Ho, P.T.P., Moran, J.M., & Rodríguez, L.F., 1982 *ApJ*, 262, 619
- Ho, P.T.P., Vogel, S.N., Wright, M.C.H., & Haschick, A.D., 1983 *ApJ*, 265, 295
- Hughes, V.A., & Wouterloot, J.G.A., 1984 *ApJ*, 276, 204
- Kawamura, J.H., Hunter, T.R., Tong, C.-Y. *et al.*, 1999 *PASP*, 111, 1088
- Laurini, S., Schilke, P., Beuther, H., & Menten, K.M., 2005 *this volume*
- Menten, K.M. & Reid, M.J., 1995 *ApJL*, 445, 157
- Minier, V., Booth, R.S., & Conway, J.E., 2000 *A&A*, 362, 1093
- Reid, M.J., & Menten, K.M., 1997 *ApJ*, 476, 327
- Rodríguez, L.F., Ho, P.T.P., & Moran, J.M., 1980 *ApJL*, 240, 149
- Schilke, P., Benford, D.J., Hunter, T.R., Lis, D.C., & Phillips, T.G., 2001 *ApJS*, 132, 281
- Schultz, A.S.B., *et al.*, 1999 *ApJ*, 511, 282
- Shepherd, D.S., Yu, K.C., Bally, J., & Testi, L., 2000 *ApJ*, 535, 833
- Sollins P.K., Hunter, T.R., Battat, J. *et al.*, 2004 *ApJL*, 616, 35
- Sridharan, T.K., Beuther, H., Schilke, P., Menten, K.M., & Wyrowski, F., 2002 *ApJ*, 566, 931
- Stolovy, S.R., Burton, M.G., Erickson, E.F., *et al.*, 1998 *ApJL*, 492, 151
- Tofani, G., Felli, M., Taylor, G.B., & Hunter, T.R., 1995 *A&AS*, 112, 299
- Torrelles, J.M., Verdes-Montenegro, L., Ho, P.T.P., Rodríguez, L.F., & Canto, J. 1993 *ApJ*, 410, 202
- Wood, D.O.S., & Churchwell, E., 1989 *ApJS*, 69, 831
- Wright, M.C.H., Plambeck, R.L., Mundy, L.G., & Looney, L. W., 1995 *ApJL*, 455, 185
- Zhang, Q., Hunter, T.R., & Sridharan, T.K., 1998 *ApJL*, 505, 151
- Zheng X.W., Ho, P.T.P., Reid, M.J., & Schneps, M.H., 1985 *ApJ*, 293, 522